The impact of indoor thermal stratification on the dispersion of human speech droplets

Article

Accepted Version

The impact of indoor thermal stratification on the dispersion of human speech droplets

Fan Liu[1, 2], Hua Qian*[,1,3], Zhiwen Luo[2], Xiaohong Zheng[1,4]

[1] School of Energy and Environment, Southeast University, Nanjing, China

[2] School of the Built Environment, University of Reading, Reading, United Kingdom

[3] Engineering Research Center of BEEE, Ministry of Education, China

[4] Jiangsu Provincial Key Laboratory of Solar Energy Science and Technology, School of Energy and Environment, Southeast University, Nanjing, China

*Corresponding author:

Postal address: No.2 Sipailou, School of Energy and Environment, Southeast University, Nanjing 210096, China.

Email address: qianh@seu.edu.cn, keenwa@gmail.com (H. Qian)

Abstract: Exhaled jets from an infected person are found to be locked at a certain height when thermal stratification exists in rooms, causing a potential high risk of disease transmission. This work is focused on the theoretical analysis of the dynamic characteristics of human speech droplets and the residual droplet nuclei in both thermally-uniform and stratified environments. Results show that most droplets generated from human speaking can totally evaporate or deposit to the ground within 1.5-2m. For small droplets of <80μm, thermal stratification shows a more significant impact on their residues. The lock-up height of the droplet nuclei is a function of droplet size and the temperature gradient, and within this lock-up layer these droplet nuclei can travel a long distance, much more than 2m. For medium droplets of 80-180μm, thermal stratification can weaken the evaporation and accelerate the deposition processes, equivalent to a higher relative humidity (RH). Accordingly, more droplets can deposit to the ground, reducing

the exposure to large droplets in close proximity to the source. Large droplets of >180μm show no dependence on stratification and RH. These findings can have implications for developing effective engineering methods to limit the spread of infectious disease.

Keywords: disease transmission; speech droplets; droplet nuclei; thermal stratification; lock-up; exposure

Practical Implications

The lock-up phenomenon of exhaled pollutants caused by indoor thermal stratification could cause a potential high risk of disease cross-infection. There is a clear need to understand the dispersion of droplets and droplet nuclei in a non-uniform indoor environment. This work is designed to illustrate in detail how thermal stratification affects disease transmission via droplets or droplet nuclei while speaking, so as to tackle the relative importance of the droplets and droplet nuclei for disease transmission in thermally-stratified indoor environments, especially in some public spaces. These findings are expected to be useful for developing engineering methods to control infectious disease transmission via large droplets or airborne routes.

Nomenclature

b	jet half width (m)
c	exhalation concentration (%)
C_d	drag coefficient (C_d=1.3)
c_p	specific heat of the droplet [J/(kg·K)]
d	droplet diameter (m)

1	D	binary diffusion coefficient (m^2/s)
2	E	entrainment rate
3	F_D	jet drag
4	g	acceleration of gravity (g=9.8m/s^2)
5	I_d	evaporation rate (kg/s)
6	K_g	thermal conductivity of the gas [W/(m·K)]
7	L_V	latent heat of vaporization (kJ/kg)
8	M	momentum flux (m^4/s^2)
9	M_v	molecular weight of vapor
10	Pr	Prandtl number
11	p_c	critical pressure (p_c=22.103MPa)
12	p_v	vapor pressure (Pa)
13	r	radial distance (m)
14	Re	Reynolds number
15	s	axial distance (m)
16	Sc	Schmidt number
17	Sh	Sherwood number
18	t	time (s)
19	T	temperature (℃)
20	T_{atm}	temperature of ambient air under standard atmosphere (℃)
21	T_c	critical temperature (T_c=647.35K)
22	x	horizontal coordinate (m)

y	vertical coordinate (m)
u	exhalation velocity (m/s)
Q	volume flux (m^3/s)
Nu	Nusselt number
J	buoyancy flux (m^4/s^3)
Q_c	tracer mass flux (m^3/s)

Greek symbols

α	entrainment coefficient (α_1=α_3=0.055, α_2=0.6, α_4=0.5)
θ	vertical angle of jet above horizontal x axis (rad)
ρ	density of exhalation airflow (kg/m^3)
ρ_{atm}	density of ambient air under a standard atmosphere (kg/m^3)
ρ_a	density of ambient air (kg/m^3)
ρ_c	centerline density of jet flow (kg/m^3)
λ	dispersion ration (λ=1.6)
μ	dynamic viscosity of the gas (Pa·s)

Subscripts

a	ambient air
c	on the centerline trajectory
g	exhaled gas
p	droplet particle
s	on the droplet surface
∞	at distance from the droplet

1. Introduction

The main motivation of the work stems from the great concern about respiratory infectious disease transmission, such as SARS in 2003 and MERS in 2012, within the public healthcare community[1-3]. Recently, the worldwide outbreak of a novel coronavirus disease (COVID-19) has reiterated the importance of studying the transmission of infectious diseases[4,5]. It has been well recognized prior to the current pandemic that respiratory viruses can be transmitted via droplets that are generated by coughing or sneezing [6,7]. It is less known that normal speaking also produces thousands of oral fluid droplets with a broad size distribution (1-1000μm)[8], which may be implicated in the person-to-person transmission of viruses. There is strong evidence now, however, that many infected individuals who transmit COVID-19 are either mildly or non-symptomatic (with no coughing or sneezing to any appreciable extent)[9,10]. Most recently, epidemiologists led by Shaman *et al.*[11] claimed that 79% of the actual infected cases were infected by individuals with "mild, limited, or no symptoms". Aerosols generated by asymptomatic individuals during normal speaking are increasingly considered to be a likely mode of disease transmission, something which has not received sufficient attention. Notably, the possible role of small speech droplets (<100μm) and their residuals after evaporation that could potentially remain airborne for extended periods of time has not been widely appreciated. Therefore, there is an urgent need to explore the dynamic characteristics of speech droplets and droplet nuclei, and their potential importance in disease transmission. This is of practical importance when making containment policies to mitigate the spread of disease, especially in some public places where asymptomatic infected individuals may be found.

Many studies exist using theoretical analyses[12-15], experiments[16-21] and computational fluid

dynamics (CFD)[22-26] to understand the dispersion of exhaled droplets. From these studies, it is noted that the dynamic characteristics of respiratory droplets are likely to be a function of the generation process, size distribution, and the environmental conditions. To be specific, the size variation and the dispersion of droplets are significantly affected by respiratory activities[8,22], thermal plumes[27-29], and indoor air flow patterns[25-27,30], etc. Among these factors, the indoor air flow patterns, e.g. natural ventilation (NV), mixing ventilation (MV), displacement ventilation (DV), downward ventilation (DnV), and under-floor air distribution (UFAD), have been recognized as an important element that distinctively affects the transmission risk via exhaled droplets or droplet nuclei due to different air distribution patterns and supply flow rates. In the experimental work of Qian *et al*.[27], it was found that in a room with MV the air temperature and airborne pollutants were generally well mixed, in which case the exposure risk to exhaled pollutants was close to that in exhaust. However, in some indoor environments, such as buoyancy-driven ventilated spaces with DV[31,32], UFAD[33,34], and/or NV[35,36], the air temperature is vertically stratified because the low-momentum air supply is attached to the floor, which is more likely to be seen in public places like shopping centers, railway waiting rooms and the rebuilt Fangcang hospital. In such environments, the exhalation airflow and airborne pollutants were found to be easily trapped at a certain height and were able to penetrate a very long distance along the exhalation direction, which was referred to as the lock-up phenomenon, as reported in previous studies[21,27,30,37,38]. Bjørn and Nielsen[17] observed that if the temperature gradient was sufficiently large, the lock-up layer of the exhaled airborne pollutants could settle at breathing height, leading to a high inhalation risk for exposed people. Liu *et al*.[30] proposed a theoretical model to predict the exposure risk of susceptible people and found that the thermal

stratification greatly weakened the decay of the exhaled pollutant concentration in the lock-up layer, thereby increasing the cross-infection range. This ventilation-induced airborne transmission may be one important reason for the reported cluster outbreak cases in public places[27,39,40]. In these studies, the exhaled contaminants were simplified as droplet nuclei (≤5μm) that would closely follow the air stream, without considering the evaporation process before the formation of droplet nuclei. However, the evaporation process has proved to be significant for the dispersion of larger droplets (e.g. 50-100μm)[14,24], which cannot be overlooked. Furthermore, how far the droplets can travel and when they transform into droplet nuclei is largely related to the environmental conditions[13-15,24]. However, how to quantify the impact of the temperature stratification on the dispersion of the exhaled droplets remains unknown. The present work aims at a basic study of the evaporation and motion of the droplets and the subsequent dispersion of the dried-out droplet nuclei, so as to explain the possibility that the airborne transmission occurs indoors while speaking, especially in a non-uniform environment.

In the classical study on respiratory infectious disease transmission, Wells[41] firstly identified that small droplets of <100μm evaporated faster than they settled, in which case the dried-out infectious droplet nuclei remained suspended in air and would be carried over a long distance. Meanwhile, droplets of >100μm rapidly settled out of air faster than they evaporated, with the infective range being within a short distance from the source. These findings resulted in a dichotomous classification between large and small droplets (or droplets and aerosols). In addition, the well-known Wells evaporation-falling curve of droplets is significant in understanding the transmission routes. Based on Wells's work, Xie *et al.*[14] simplified the respiratory droplets as pure water droplets and revisited the evaporation-falling curves for

different respiratory activities and RH using the empirical formulas for an isothermal jet flow. Afterwards, Liu *et al*.[42] estimated the residue size of a respiratory droplet using equilibrium theory and explored the effects of initial salt concentration, solid volume ration, and RH on droplet nucleus size and droplet dispersion. Subsequently, the impacts of turbulent fluctuation were also discussed by Wei and Li[13] by using the particle tracking model. Recently, Chen *et al*.[43] clarified the difference between the exposure to exhaled droplets via the short-range airborne and large droplet sub-routes using a model of droplet dispersion/deposition/inhalation. They emphasize the important role of the droplet dynamics in the transmission of respiratory diseases. Research on respiratory infection via human exhaled pathogen-laden droplets is a multi-faceted study of building environment, jet theory, multiphase flow and infectious diseases. However, all these theoretical models of the evaporation process of exhaled droplets merely focused on the jet flow itself and ignored the indoor airflow patterns. Ji *et al*.[24] compared the evaporation and dispersion of respiratory droplets in MV and DV using CFD. It was found that DV worked as a barricade for the evaporation of middle droplets (e.g. 50μm), preliminarily indicating a significant impact of a non-uniform indoor environment on the dispersion of exhaled droplets. A detailed explanation for the mechanism of the dispersion of exhaled droplets and the residues in thermally-stratified indoor environments needs to be studied further.

The importance of identifying the impact of thermal stratification on the dispersion of exhaled droplets and droplet nuclei is obvious. In a companion paper, an integral model was proposed for characterizing human exhalation so as to obtain the distribution of the exhaled gas contaminants and differentiate the exposure modes of the susceptible individuals, in which both the ambient velocity and ventilation-induced temperature stratification were considered[30]. The

applicability of this comprehensive model of human exhalation airflow and particle transport has been validated by a reduced-scale model in our water tank experiments[21]. In this work, the integral model is combined with the dynamics of droplets to explore the impact of thermal stratification on the dispersion of speech droplets and droplet nuclei, so as to clarify the potential effects of the lock-up phenomenon on disease transmission via droplets or droplet nuclei. There are significant implications for improving ventilation strategy to mitigate the spread of disease.

2. Mathematical models

The models in this work include an estimation of the drying-out process and the dispersion of both droplets/droplet nuclei as affected by indoor thermal stratification. The calculation includes three parts: the ambient air, the exhaled air, and the exhaled droplets. The exhaled droplets move and transform into droplet nuclei in the combined background of exhaled air and ambient air with a thermal stratification. We adopted an integral model of expiratory jet flow and dynamic equations for a single droplet. We are interested in how the speech droplets and the airborne residuals disperse in indoor environments with and without thermal stratification.

2.1 Mathematical model for exhalation jet flow in thermally stratified environments

The exhalation airflow from the oral cavity is often treated as a steady turbulent round jet oriented in the x-direction (i.e. θ_0=0), and there is no inhalation but only continuous exhalation in previous studies [13,14,30,42], as shown in Fig. 1. The exhaled air temperature is generally higher than the indoor air temperature. In this case, the non-isothermal turbulent jet is dominated by the buoyancy and so curves upwards. The jet flow includes an initial flow establishment zone and an established flow zone. The establishment zone is a transition region that lacks self-

similarity because the initial unsheared profiles change with the peripherally growing axisymmetric mixing layers until becoming the final jet profiles. An empirical value of $Le \approx 5D$ is used here to specify the length of this zone from the oral cavity [44], where D is the diameter of the jet efflux. In the established zone, the parameters on the cross-sectional plane follow the Gaussian profiles [45], as shown below.

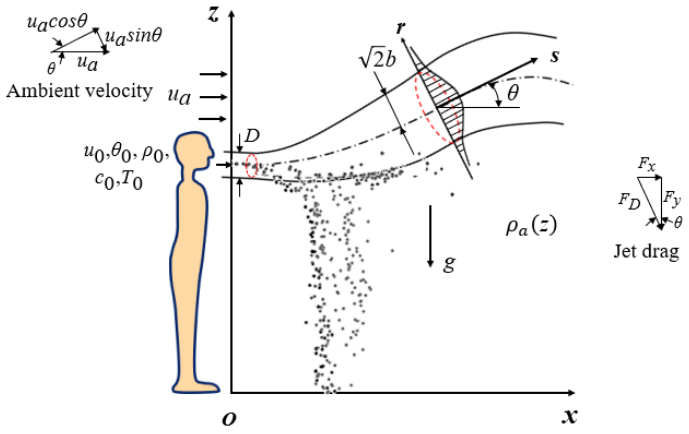

Fig. 1 Illustration of the expiratory jet flow in a thermally stratified environment

$$u = u_c exp\left(\frac{-r^2}{b^2}\right) + u_a cos\theta \quad (1)$$

$$\frac{\rho_a(z) - \rho(z)}{\rho_a(z) - \rho_c} = exp\left(\frac{-r^2}{\lambda^2 b^2}\right) \quad (2)$$

$$c = c_c exp\left(\frac{-r^2}{\lambda^2 b^2}\right) \quad (3)$$

$$T = T_c exp\left(\frac{-r^2}{\lambda^2 b^2}\right) + T_a(z) \quad (4)$$

By integrating Eqs. (1) - (4) on the cross-sectional plane of the jet flow, the specific fluxes (the flux per unit mass) including the total volume flux (Q), momentum flux (M), buoyancy flux (J), tracer substance flux (Q_c) and flux of heat content (Q_T) in the turbulent jet zone are obtained[45]:

$$Q = 2\pi \int_0^{R_j} u r dr = \pi b^2 (u_c + 2u_a cos\theta) \quad (5)$$

$$M = 2\pi \int_0^{R_j} u^2 r dr = \frac{1}{2} \pi b^2 (u_c + 2u_a cos\theta)^2 \quad (6)$$

$$J=2\pi\int_0^{R_j}\frac{(\rho_a-\rho)g}{\rho_{a0}}urdr=\pi b^2\left(u_c\frac{\lambda^2}{\lambda^2+1}+\lambda^2u_a\cos\theta\right)\frac{(\rho_a-\rho_c)g}{\rho_{a0}} \tag{7}$$

$$Q_c=2\pi\int_0^{R_j}ucrdr=\pi b^2\left(u_c\frac{\lambda^2}{\lambda^2+1}+\lambda^2u_a\cos\theta\right)c_c \tag{8}$$

$$Q_T=2\pi\int_0^{R_j}u(T-T_a)rdr=\pi b^2\left(u_c\frac{\lambda^2}{\lambda^2+1}+\lambda^2u_a\cos\theta\right)T_c \tag{9}$$

in which, $R_j=\sqrt{2}b$ defines a local velocity excess of 14% and a scalar value of 25% of the centerline values, as measured by Chu[46] with the purpose of defining the turbulent jet flow boundary within which the actual transport and mixing processes occur. In Eq. (7), the buoyancy flux is dependent on a stable density distribution of ambient air $\rho_a(z)$ (as shown in Fig. 1) in a thermally-stratified environment, which is determined by the temperature distribution in the vertical z-direction.

The integral equations are formulated in terms of the above flux quantities at an element ds on the central trajectory and the conservation principles for volume (continuity), momentum components in the directions x and y, buoyancy, tracer substance, and heat content are satisfied:

$$\frac{\mathrm{d}Q}{\mathrm{d}s}=E \tag{10}$$

$$\frac{\mathrm{d}}{\mathrm{d}s}(M\cos\theta)=Eu_a+F_D\sin\theta \tag{11}$$

$$\frac{\mathrm{d}}{\mathrm{d}s}(M\sin\theta)=\pi\lambda^2b^2\frac{(\rho_a-\rho_c)g}{\rho_{a0}}-F_D\cos\theta \tag{12}$$

$$\frac{\mathrm{d}J}{\mathrm{d}s}=Q\frac{g}{\rho_{a0}}\frac{\mathrm{d}\rho_a}{\mathrm{d}y}\sin\theta \tag{13}$$

$$\frac{\mathrm{d}Q_c}{\mathrm{d}s}=0 \tag{14}$$

$$\frac{\mathrm{d}Q_T}{\mathrm{d}s}=-Q\frac{\mathrm{d}T}{\mathrm{d}z}\sin\theta \tag{15}$$

Here, the entrainment rate E is specified as the additive contributions of the different streamwise and azimuthal shear mechanisms that lead to the entrainment of the surrounding fluid into the turbulent jet flow, defined as[47]:

$$E=2\pi bu_c\left(\alpha_1+\alpha_2\frac{\sin\theta b(\rho_a-\rho_c)g}{u_c^2\rho_{a0}}+\alpha_3\frac{u_a\cos\theta}{u_c+u_a}\right)+2\pi bu_a\sin\theta\alpha_4|\cos\theta| \tag{16}$$

The jet drag F_D in Eq. (12) is specified by analogy to the flow (ambient flow) around a cylindrical solid body (jet flow) [47]:

$$F_D=C_d 2\sqrt{2}b\frac{u_a^2 sin^2\theta}{2} \tag{17}$$

in which $u_a sin\theta$ is the ambient velocity component transverse to the jet flow, and $2\sqrt{2}b$ the diameter of jet flow (as shown in Fig. 1).

The geometry of the centerline trajectory is determined by

$$\frac{dx}{ds}=cos\theta \tag{18}$$

$$\frac{dz}{ds}=sin\theta \tag{19}$$

2.2 Droplet transformation and motion

The calculation for the evaporating and moving droplets is based on the existing models developed by Wei and Li[20], with the governing equations for motion, mass flux, and heat content listed below.

$$\frac{d\vec{u_p}}{dt}=\vec{g}\left(1-\frac{\rho_g}{\rho_p}\right)-\frac{3C_d\rho_g}{4d_p\rho_p}\left|\vec{u_p}-\vec{u_g}\right|\left(\vec{u_p}-\vec{u_g}\right) \tag{20}$$

$$-\frac{dm_p}{dt}=I_d=-\frac{2\pi p d_p M_v D_\infty CSh}{RT_\infty}ln\left(\frac{p-p_{va}}{p-p_{v\infty}}\right) \tag{21}$$

$$m_p c_p\frac{dT_p}{dt}=\pi d_p^{\,2}K_g\frac{T_\infty-T_p}{r_p}Nu-I_d L_V \tag{22}$$

in which the drag coefficient C_d is determined by the Reynolds number Re_p [13]:

$$C_d=\begin{cases}\frac{24}{Re_p}\left(1+\frac{1}{6}Re^{2/3}\right), & Re_p<1000\\ 0.424, & Re_p\geq 1000\end{cases} \tag{23}$$

with the Reynolds number Re_p defined as

$$Re_p=\rho_g d_p\left|\vec{u_p}-\vec{u_g}\right|/\mu \tag{24}$$

Here, C is a correction factor because of the temperature dependence of the diffusion coefficient, which is given by

$$C=\frac{T_\infty-T_p}{T_\infty^{\lambda-1}}\frac{2-\lambda}{T_\infty^{2-\lambda}-T_p^{2-\lambda}} \tag{25}$$

The Sherwood number and the Schmidt number are given by

$$Sh=1+0.3Re_p^{1/2}Sc^{1/3},\ Sc=\mu/\rho_g D \tag{26}$$

The Nusselt number and the Prandtl number are given by

$$Nu=1+0.3Re_p^{1/2}Pr^{1/3},\ Pr=c_g\mu/K_g \tag{27}$$

The vapor pressure at the droplet surface p_{va} is assumed to be saturated, determined by the droplet temperature T_p. For a given temperature T, there is a saturation vapor pressure p_{vas}, as described in Eq. (28)[48], and $p_{v\infty}=p_{vas}\cdot\mathrm{RH}$ is the partial vapor pressure distant from the droplet, RH the relative humidity of local air.

$$ln\frac{p_{vas}}{22050000}=(9.031645+2.993\left(1-\frac{T}{647.1}\right)^{1.89}+47.5\left(1-\frac{T}{647.1}\right)^{5.67})ln\frac{T}{647.1} \tag{28}$$

The displacement of the droplet is

$$\frac{\mathrm{d}\overrightarrow{x_p}}{\mathrm{d}t}=\overrightarrow{u_p} \tag{29}$$

In the calculations, the average expiration air velocity at the mouth when speaking is 3.9 m/s as measured by Chao *et al*.[49], in which subjects were asked to count from "1" to "100" in English. The exhaled air temperature is assumed to be 35.1℃, averaged between patients with asthma and control subjects[50], and the typical room temperature is 25℃ in a thermally uniform environment, with a vertical temperature gradient of 2℃/m in a thermally stratified environment. The proportion of water vapor in exhaled air is 1.1%, the RH of indoor air is 50%, and atmospheric pressure is 101,325Pa. The infector is assumed to be standing and droplets are exhaled at a height of 1.75 m.

Droplets are assumed to be perfect spheres that evaporate to a final diameter due to the existence of insoluble solids[42]. For the assumed droplet composition (here physiological saline

solution (0.9 w/v)), the final droplet nucleus size is 32.5% of the initial droplet diameter[13,42]. The residual droplet nuclei will continue to be carried along with the exhaled airflow.

The above models are solved numerically by a self-written code using the fourth-order Runge-Kutta method in MATLAB R2017a (MathWorks Inc., Natick). The local parameters, such as air velocity, temperature and density on the droplet trajectory need to be updated at every time-step during a numerical calculation. For different droplet diameters, the time-step will also need to change.

3. Results

3.1 Model validations

The above models are firstly validated by the published experimental data and compared with the empirical formulas, followed by their applications to discuss the impact of an indoor stratified environment on the dispersion of speech droplets and droplet nuclei.

Smolík *et al*.[51] carried out an experiment to observe the heat and mass transfer of a suspended droplet, in which a free-stream velocity of 0.203m/s was produced by a nozzle. The same experimental conditions are repeated in the present integral model and the empirical formulas that were frequently used in previous work[13,14,42], respectively, with the results shown in Fig. 2. It is found that the integral model result shows a very good agreement with the experimental data, while a distinct deviation exists between the experimental data and the predictions from the empirical formulas. This is because the free-stream velocity of the ambient air is not considered in empirical formulas, causing a longer evaporation time for the droplets. In addition, when thermal stratification exists indoors, the buoyancy of the exhaled jet flow is

affected by the ambient temperature (density) gradient, which is also ignored in the empirical formulas.

This implies that the integral model in this work is superior in describing the evaporation and dispersion of the exhaled droplets in both thermally-uniform and stratified indoor environments.

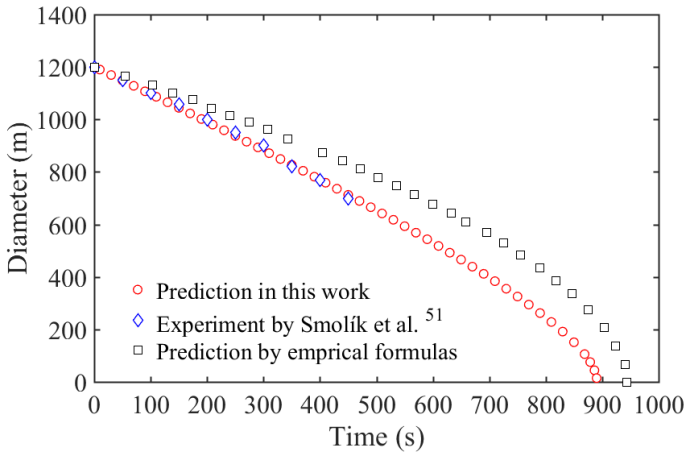

Fig. 2 Comparison of the predicted droplet diameter using the present model, empirical formulas and experimental results from Smolík *et al.* [51]. Parameters in the experiment setups were: air temperature=297K, RH=35%, droplet temperature=287K, and initial droplet size=1.2 mm.

3.2 Droplet nuclei of small droplets (<80μm) are locked at a lower height close to breathing height at a stronger stratification

Large droplets of >200μm can rapidly deposit to the ground due to gravity, hardly affected by the environmental conditions[13,14,24]. Therefore, the impacts of thermal stratification on small droplets of <80μm and medium droplets of 80-200μm will be detailed. The results for a uniform environment ($dT/dz=0$) are included here to make a comparison. All parameters are kept constant except for the temperature gradient which ranges from 0 to 6°C/m, which covers most cases in a ventilated room.

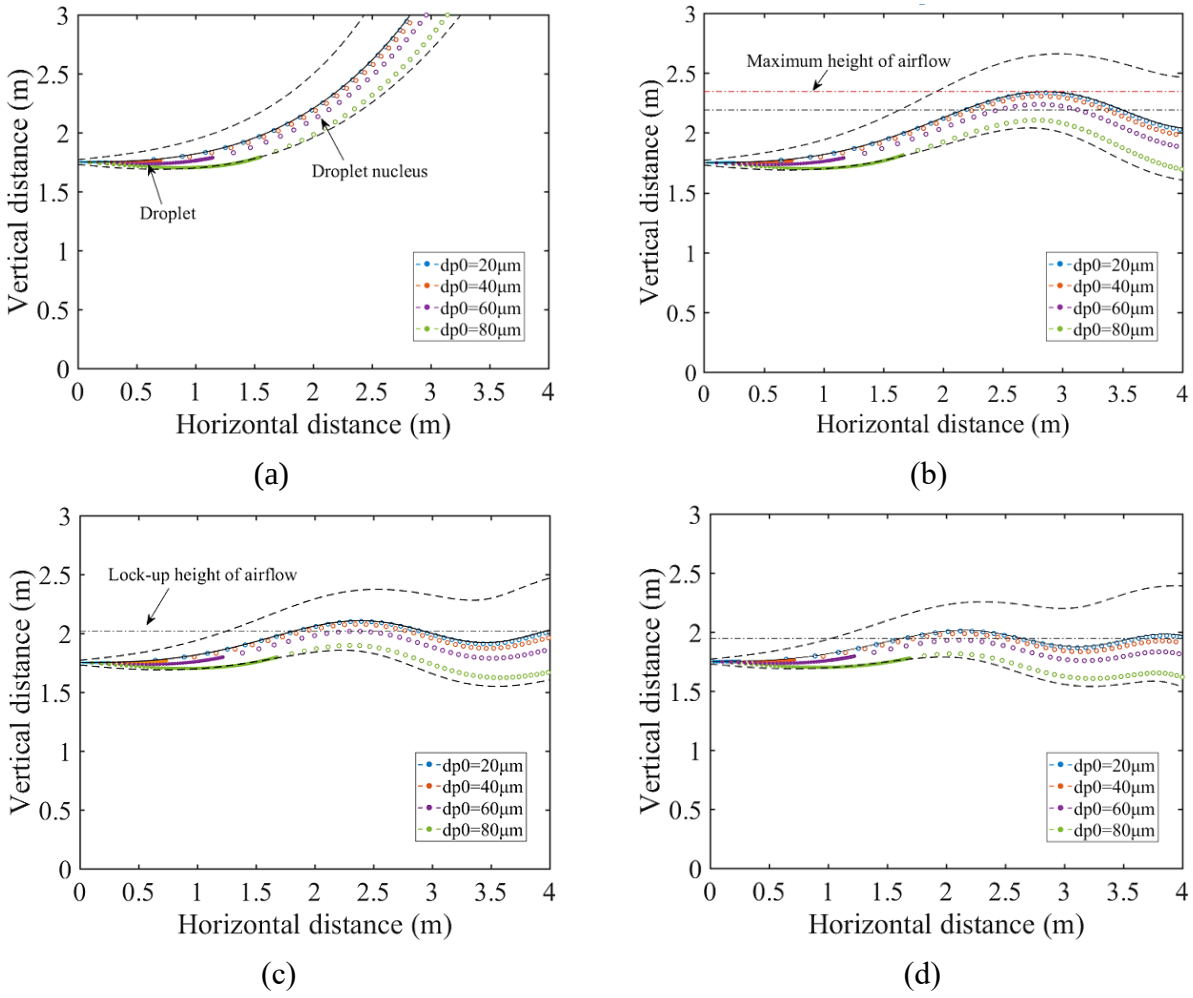

Fig. 3 Trajectories of droplets and droplet nuclei of different diameters. The jet trajectory is indicated by the black solid line, and upper/lower boundaries by the black dashed lines: (a) dT/dz=0 (uniform environment); (b) dT/dz=2°C/m; (c) dT/dz=4°C/m; (d) dT/dz=6°C/m

Fig. 3 shows the trajectories of the exhaled airflow and small droplets of <80μm in both uniform and stratified environments. It can be seen that small droplets evaporate totally within a short distance (<1.5m) while speaking, and the residual droplet nuclei continue to disperse with the airflow. In a uniform environment (Fig. 3(a)), the droplets and dried-out droplet nuclei will be kept moving upwards with the exhaled airflow, and finally be concentrated near the ceiling. Therefore, the individual exposure to airborne droplet nuclei is extremely low at a distance of >1.5 m. When a thermal stratification exists indoors, as shown in Figs. 3(b)-(d), the

dispersion of exhaled airflow and droplets becomes a little more complicated. For the exhaled airflow, the trajectories are firstly upward and overlapped, while beginning to show distinctive oscillations once being trapped by thermal stratifications, and travel long distances of up to 4m. A steeper stratification contributes to both lower lock-up and maximum heights of the exhaled airflow. This phenomenon can be explained by the temperature decay on the exhaled airflow trajectory in Fig. 4. The upward jet flow is driven by buoyancy, the result of the temperature difference (ΔT) between the rising airflow T_c and the ambient air T_a. It is found from Fig. 4 that in a stratified environment, with the rising height, ΔT decreases to 0 at some height (i.e., the lock-up height); the subsequent negative value of ΔT is induced by the continuous rising due to jet inertia until reaching its maximum height. The upward displacement of the airflow will make it cooler than the ambient air and hence it tends to fall back to the lock-up height. Conversely, the downward displacement will make the airflow warmer than the ambient air and tend to return to the lock-up layer. This process is repeated and results in the overlapped values of ΔT around 0, as shown at the end of the curves. Furthermore, Fig. 4 also shows that with a larger temperature gradient, ΔT decreases to 0 after rising a shorter distance, otherwise, it will reach a higher layer, as in the dispersion trajectories shown in Figs. 3(b-d). In an extreme case where the temperature gradient is close to 0, i.e. the ambient air tends to be thermally uniform, the jet flow will continue upwards to the ceiling, as shown in Fig. 3(a)).

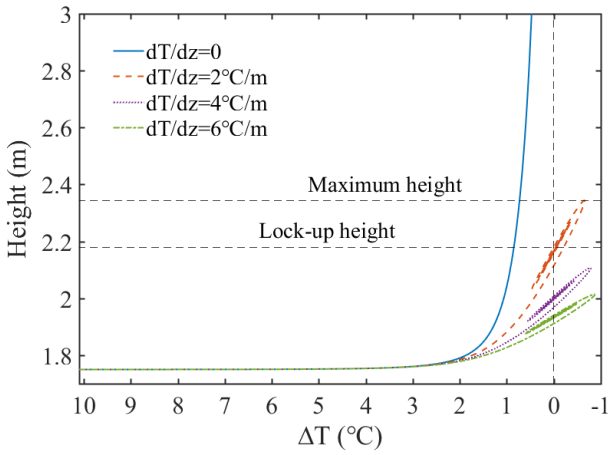

Fig. 4 Variations of the temperature difference (ΔT) on the jet flow trajectory with the temperature gradient

For the small droplets (<80μm), similar dispersion trends before complete evaporation are observed from Figs. 3(a-d). They are less affected by the thermal stratification, until the droplets shrink to a critical size (32.5% of their initial size). The gravity, buoyancy and the drag force because of local exhaled air resistance of the droplets in Eq. (20) are calculated and presented in Fig. 5. It is found that in the evaporation process, the drag force (shown in Fig. 5(b)) dominates the droplet motion, larger by two orders than the gravity and buoyancy (shown in Fig. 5(a)). When the drag force tends to 0, i.e. the droplet velocity approaches the local air velocity, it means that the droplets or their residuals are fully carried by the exhaled airflow. Accordingly, the lock-up phenomenon and oscillation occur in the subsequent dispersion of droplet nuclei. In this case the airborne droplet nuclei can travel up to 4m, much more than 2m. It should be noted that the lock-up phenomenon of the droplet nuclei is different from that of the exhaled airflow. The lock-up and maximum heights of the airborne residuals are found to be dependent not only on the temperature gradient, but also on the initial size of the droplets/droplet nuclei.

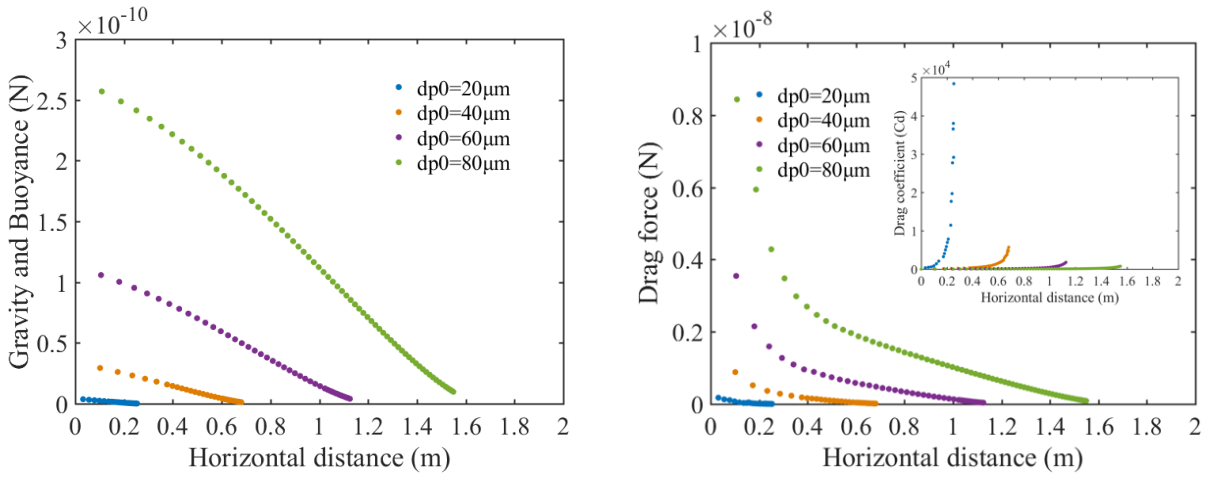

(a) (b)

Fig. 5 Forces acting on droplets of <80μm with dispersion distance (d*T*/d*z*=2°C/m): (a) gravity and buoyancy (the first term on the right-hand side in Eq. (20)); (b) drag force due to exhaled air resistance (the second term on the right-hand side in Eq. (20))

Fig. 6 summarizes the maximum and lock-up heights of the trajectories of the exhaled airflow and the droplet nuclei based on droplet initial sizes and temperature gradients. As the indoor temperature stratification increases from 1°C/m to 6°C/m, the maximum and lock-up heights of the exhaled airflow decrease from 2.73m to 2.01m and from 2.47m to 1.94m respectively, in a power law relationship. Accordingly, the lock-up and maximum heights of the droplet nuclei also show the same trends. In addition, given the same thermal stratification, the lock-up height of the droplet nuclei shows a clear relationship with the initial size of the droplet. It can be found that the residuals of 20μm droplets will travel to a great height driven by the airflow. As the droplet size increases, the droplet nuclei will tend to leave the jet flow, which is well illustrated by the droplets of 80μm that disperse close to the lower boundary of the jet flow. As seen in Fig 6(a), the nuclei of 80μm droplets are trapped at a lower height of <2 m when the temperature gradient increases to 1.5°C/m. In this case, airborne droplet nuclei could travel a

long distance (up to 4m) within people's breathing zone, causing a higher inhalation risk for susceptible people. The regression coefficients in the power relations for the exhaled airflow and droplet nuclei are given in Tables 1 and 2, respectively. This finding suggests that for small droplets of <80μm, the airborne infection risk caused by the dried-out droplet nuclei is more significant than that caused by the droplets themselves. The quantitative relationships could be beneficial for improving indoor ventilation design to keep the exhaled airborne aerosols away from the breathing zone of susceptible individuals.

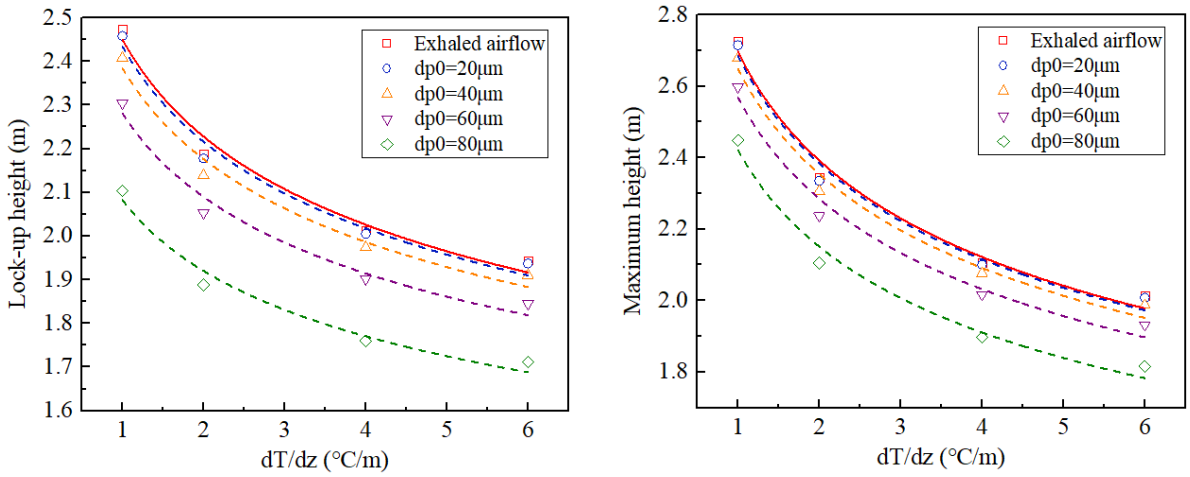

Fig. 6 (a) Maximum height and (b) lock-up height of the trajectories of the exhaled airflow and dried-out droplet nuclei

Table 1 Regression coefficients of the power law relation for the lock-up height:

$$y_L=(a+b\cdot d_{p0})\cdot(dT/dy)^c.$$

	Coefficient a	Coefficient b	Exponent c	R^2
Exhaled airflow	2.450	0	-0.137	0.982
Droplet nuclei	2.557	-0.005	-0.128	0.961

Table 2 Regression coefficients of the power law relation for the maximum height:

$$y_M=(a+b\cdot d_{p0})\cdot(dT/dy)^c.$$

	Coefficient a	Coefficient b	Exponent c	R^2
Exhaled airflow	2.697	0	-0.173	0.985
Droplet nuclei	2.941	-0.007	-0.201	0.840

3.3 Medium droplets (80-180μm) evaporate more slowly and deposit more quickly with increasing thermal stratification

As stated above, the thermal stratification can trap the droplet nuclei at lock-up heights by affecting the airflow evolution. While larger droplets can escape from the jet flow region and travel in the ambient air, so the thermal stratification acts directly on droplet evaporation and motion. The travelling distances for the medium droplets, which are defined as the dispersion distances of droplets before shrinking into droplet nuclei, are calculated and plotted in Fig. 7. It can be seen from Fig. 7(a) that the droplets of <90μm can travel a longer distance along the exhalation direction with the airflow. However, with the increasing size, the droplets begin to escape from the airflow region and deposit due to gravity, accordingly, the horizontal distance becomes shorter. Most of the exhaled droplets travel a distance of <1.5m, indicating that the speech droplets can totally evaporate or settle in close proximity to the source infector, a process which is unaffected by thermal stratification. However, the falling distance in Fig. 7(b) shows an obviously increasing trend with the temperature gradient, with different droplet sizes also contributing to the different falling distances. Notably, the droplets of 150μm fall 1.5m in a uniform environment and remain suspended in air, while traveling 1.75m (depositing to the ground) in stratified environments. Being suspended or depositing to the ground is determined by the evaporation of droplets. As given in Eqs. (21-22), droplet evaporation is in nature a heat

and mass transfer process in the exhaled air or ambient air, driven by the temperature difference (ΔT_p) and pressure difference (Δp) between the droplet surface and local air distant from the droplet, respectively. Fig. 8 shows the variations in the falling process. It can be found that there is no difference in the driving potentials for the droplet evaporation in the initial stages. This is because the droplets firstly travel within the jet flow region after being expelled, in which the thermal stratification has little impact on the driving potentials. When the droplets escape from the jet and settle in the air, the driving potentials obviously decrease with the stratification intensity, weakening the evaporation of droplets.

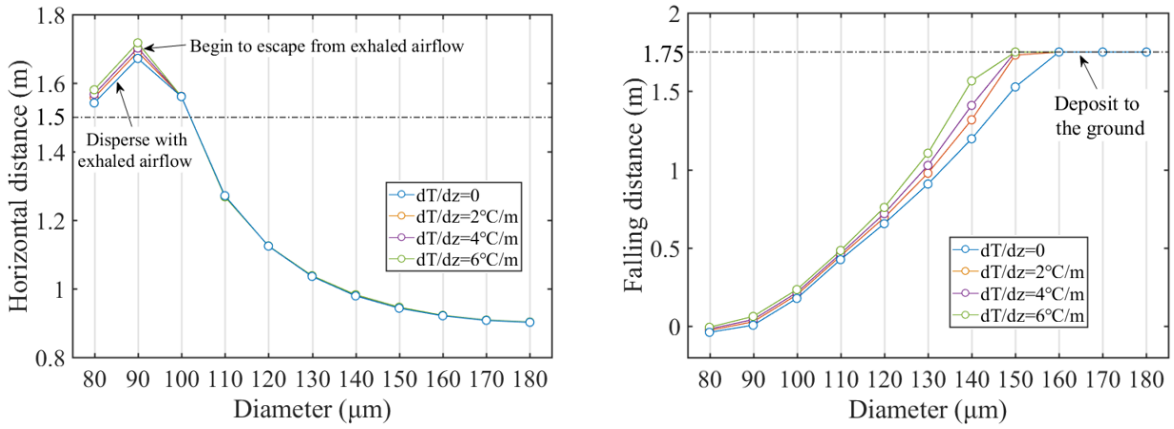

(a) (b)

Fig. 7 Travelling distance of droplets with different initial sizes at different temperature gradients: (a) horizontal distance; (b) falling distance

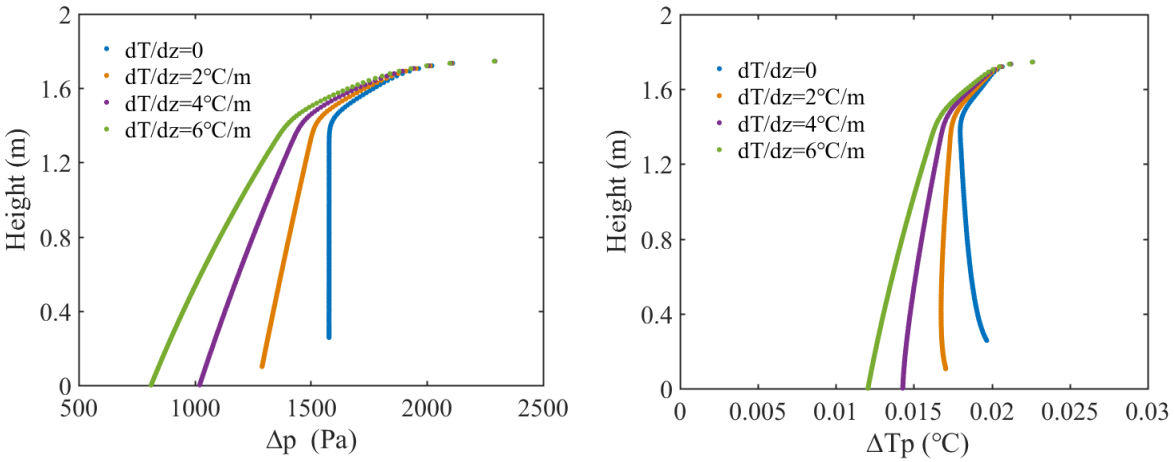

(a) (b)

Fig. 8 Variations of (a) vapor pressure difference and (b) temperature difference in the falling process of 150μm droplets

To qualify the above impact on the evaporation process of medium droplets (80-180μm), the variation in dimensionless droplet diameter (the ratio of droplet diameter to initial diameter) is compared for the droplets in Fig. 9(a). It is assumed that all exhaled droplets share the same initial solid volume ratio (32.5%)[13], so the final dimensionless diameter value remains constant for each size. Results show that the 80μm droplet shrinks rapidly within 2s, and 180μm droplet falls quickly onto the ground after approx. 3.2s. Thermal stratification shows a remarkable effect on the evaporation process of the 100-150μm droplets. Specifically, the curves of droplets >80μm begin to diverge after about 1s, and a longer time is needed for total evaporation of droplets as the temperature gradient increases. Most obviously, the 150μm droplet can completely evaporate before settling in a weak thermal stratification, however, as the stratification becomes steeper, the droplets shrink so slowly that they drop down to the floor before total evaporation. In addition, the larger the temperature gradient is, the less time it takes for the droplet to deposit.

The evaporation time (curve AB) and deposition time (curve BC) are plotted with the temperature gradient in Fig. 9(b). The intersection of the evaporation time and falling time curves (point B) indicates the largest droplet that can completely evaporate in the air after being released from a height of 1.75m. It is found that as the temperature gradient increases, the intersection point B (155μm) moves to the left point B' (142μm) in a stratified environment, indicating a transition from evaporation to deposition for the droplets of 142-155μm. That

means that, under an intense stratification, more droplets will deposit to the ground, thereby reducing the exposure to large droplets in close proximity. But in this case, the droplet nuclei of small droplets will be trapped within people's breathing zone (see Fig. 3(d)), increasing the exposure risk to airborne droplet nuclei over a long range.

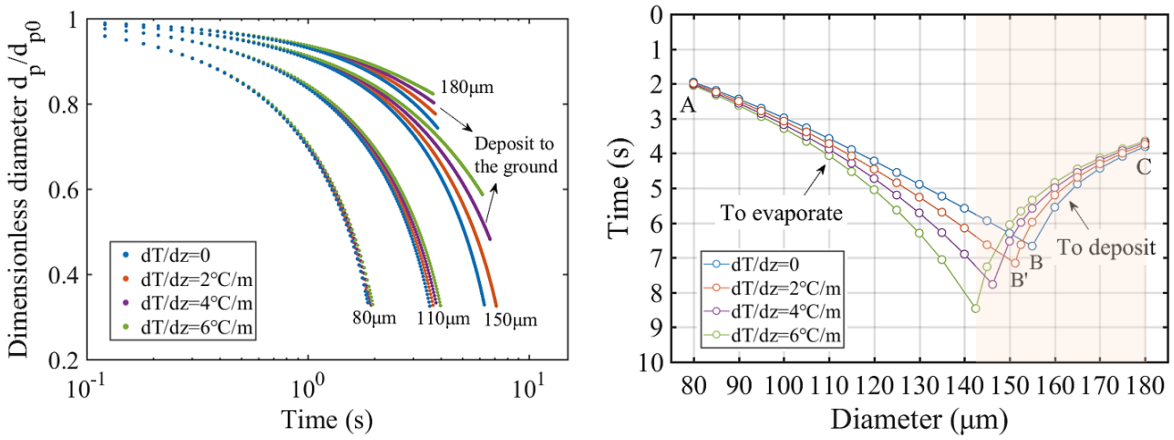

(a) (b)

Fig. 9 Variations of droplet diameter with time under different thermal stratifications: (a) dimensionless diameter with time; (b) revisited Wells evaporation-falling curves

3.4 A stronger thermal stratification works equivalently to a higher RH for medium droplets

RH is proved to have a great impact on droplet evaporation and falling rate[13,14,24]. The calculations are performed here at RHs of 50%, 60%, 70% and 80% in a thermally uniform environment so as to compare the impact of RH with that of thermal stratification. Fig. 10 shows the trajectories of exhaled droplets and droplet nuclei with RH. It can be found that the dispersion of droplets smaller than 40μm and their droplet nuclei are hardly affected by RH, and the lock-up layer remains unchanged. Droplets of 200μm deposit quickly, also independent of RH. However, the droplets of 80μm that disperse with the exhaled airstream begin to escape from the jet region when RH increases to 80%. With the current model, RH does not change

the velocity of the exhaled airflow, so it cannot influence the droplet velocity directly as the thermal stratification does; instead, its effect is through the evaporation rate. Fig. 11 shows the driving potentials for 120μm droplet evaporation with increasing RH. It can be observed that a larger RH contributes smaller temperature and pressure differences between the droplet surface and its surrounding air. Similar to an intensive thermal stratification, RH can also hinder droplet evaporation. However, what makes it different to thermal stratification is the strong impact of RH on the driving potentials from the beginning of the droplet evaporation. This means that more droplets are affected and evaporate more slowly at a higher RH, and finally deposit to the ground.

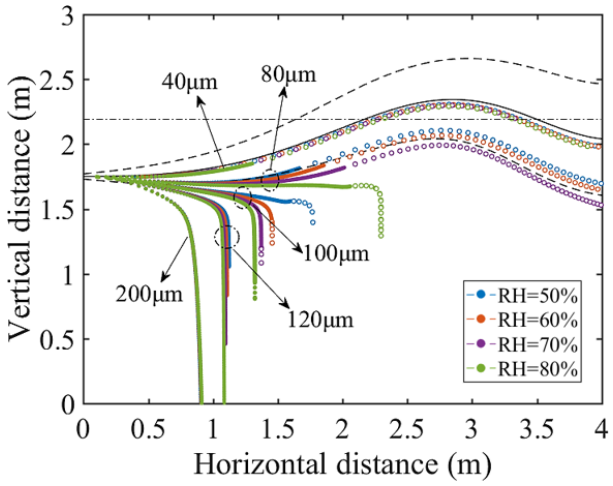

Fig. 10 Trajectories of droplets and droplet nuclei of different diameters at different RHs

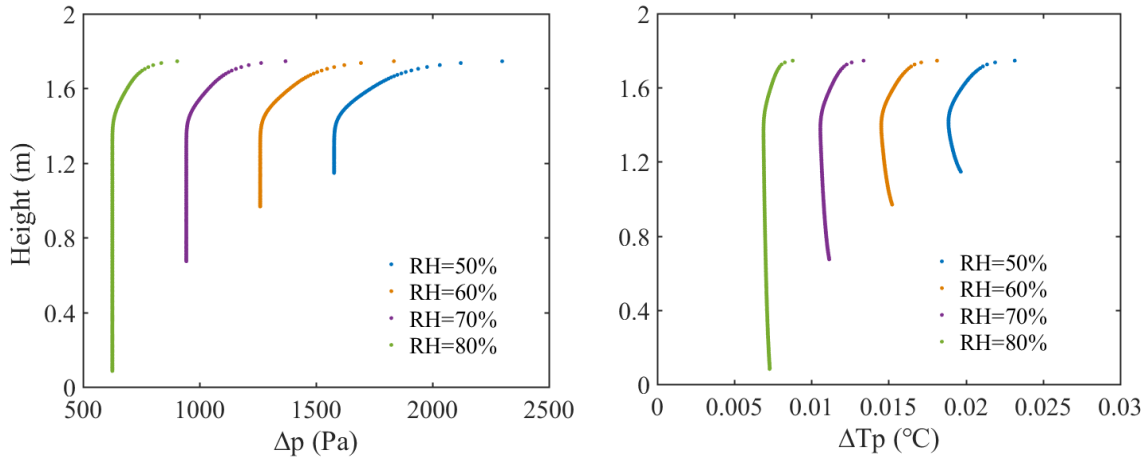

(a) (b)

Fig. 11 Variations of (a) vapor pressure difference and (b) temperature difference in the falling process of 120μm droplets

The impact of RH on the evaporation and falling time of droplets is given in Fig. 12. It is noted that for medium droplets of 40-180μm, a high RH can both reduce the evaporation and accelerate the deposition. As a result, the droplet sizes at the curve intersections are found to be 160, 145, 135 and 120μm at 50%, 60%, 70% and 80%, respectively, decreasing with RH. The calculations are consistent with the predicted results using empirical formulas in the literature[14]. This means that a large RH shows a similar, but a little stronger, impact on the droplet evaporation and deposition than does the thermal stratification. A high RH has been suggested as one of the key factors for SARS transmission in some areas[52]. However, RH shows no impact on the dispersion of airborne droplet nuclei that are easily carried by the exhaled airflow. Accordingly, the stratification-induced long-range dispersion of fine aerosols at the lock-up layer is hard to control by changing RH, in which case a high RH is ineffective at mitigating the inhalation risk from small droplets or droplet nuclei.

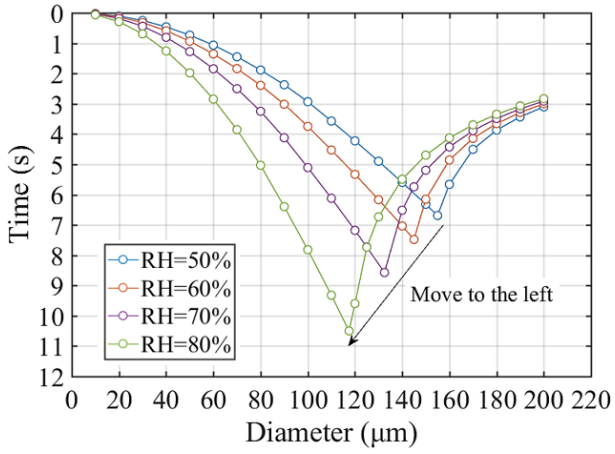

Fig. 12 Evaporation time for small droplets and falling time for large droplets at different RHs

4. Discussion

Respiratory infections occur through the transmission of virus-laden droplets and droplet nuclei exhaled from infected individuals during breathing, speaking, coughing, and sneezing. Many existing studies have focused on the strong respiratory events, such as coughing and sneezing[13,15,20,53]. However, it has been revealed that the number of droplets produced by speaking is similar to that produced by coughing[49]. Especially in the recent worldwide spread of COVID-19, it has been reported that the infection appears to be occurring via aerosols produced by asymptomatic individuals without coughing or sneezing. Therefore, transmission via pathogen-laden droplets while speaking is a potential threat to people's health, especially in public places. Our calculations show that the individual exposure to the speech droplets may happen in close proximity (<2m) to a source patient, while the exposure to the droplet nuclei may exist over a long distance (much greater than 2m), which is largely affected by indoor temperature stratification.

In this study, most of the exhaled droplets produced by speaking are found to deposit or totally evaporate within a short distance of 1.5m from the source patient; this finding is consistent with previous observations using empirical formulas[14] or the CFD simulations[12]. Notably, in the CFD simulations by Liu *et al*. [12], a periodic exhalation close to a real respiratory event was set for the targeted person, which was simplified from practical medical scanning; therefore, the consistent results validate that the simplification of the turbulent jet model in this work is reasonable and effective. A threshold distance of about 1.5m has been generally suggested to distinguish short-range modes (including the large droplet route and short-range airborne transmission) and the long-range airborne route[12]. Accordingly, a 1.5m social

distancing rule to mitigate the spread of the COVID-19 is proposed in some countries, such as China, Australia and Germany[54,55]. However, when considering the thermal stratification induced by some airflow patterns, the disease transmission via droplets or airborne droplet nuclei becomes more complicated. The present work suggests that droplet exposure can involve any size of droplets in both thermally uniform and stratified environments, and it mostly occurs at close proximity (<2m) to the source person. However, it should be noted that in stratified environments, a higher temperature gradient can weaken the evaporation and accelerate the deposition of exhaled droplets (80-180μm). This means that thermal stratification delays the transformation from 'droplet' to 'droplet nucleus', thus affecting whether a droplet is being deposited to the floor or remaining suspended in air. When there is a breathing height difference between a source person and a receiver within close proximity, such as a healthcare worker and a bed-ridden patient in a hospital ward, seated and standing patients in hospital waiting rooms, and children and adults, whether the virus is transmitted via large droplets or airborne droplet nuclei jointly depends on the height difference and the ambient temperature stratification. By revisiting the evaporation-falling curves, a similar impact of thermal stratification is found with a high RH. Both the factors can decrease the critical size corresponding to total evaporation in air and contributing to the deposition of more droplets, as a result of which the exposure to, and inhalation risk from, large droplets becomes smaller in close proximity. Accordingly, to minimize the droplet exposure risk, a social distance of >2m should be kept in public spaces, as suggested as one of the key factors for COVID-19 risk mitigation in non-healthcare public services[56].

The lock-up phenomenon is observed in the droplet nucleus dispersion, i.e. the airborne

droplet nuclei can be trapped at some height in an indoor environment and travel a long distance along the exhalation direction. However, the lock-up phenomenon of the droplet nuclei is different from that of the exhaled airflow reported in previous studies. As stated by Zhou *et al*.[38], the lock-up height of exhaled airflow is determined by the temperature gradient, and a large temperature gradient contributes a lower lock-up height. Whereas, it is found in this study that the lock-up height of the airborne droplet nuclei is a function of both temperature gradient and the initial size of the droplet, i.e., $y=(a+b\cdot d_{p0})\cdot(dT/dy)^{c}$. For susceptible people at different breathing heights, they may be exposed to droplet nuclei with different sizes; the higher the breathing height, the greater the inhalation risk from aerosols. In addition, the inhalation of the aerosols with different sizes will cause differences in deposition efficiency in the respiratory system, such as head airways (HA), the tracheobronchial region (TB) and the alveolar region (AL)[57]. Carvalho *et al*. [58] found that particles of 1-5μm are mostly deposited in AL, while those larger than 10μm are easily deposited in HA. Therefore, the evaporation and deposition characteristics of exhaled droplets is a significant foundation for exploring the dose-response rate of infectious viruses in the human respiratory tract. The findings also imply that in ventilated built environments, especially in large spaces with a dense population, such as railway stations, shopping centers, gymnasia, and hospital halls, the long-range spread of speech droplet nuclei induced by thermal stratification should receive greater attention. Improving the ventilation design, such as increasing the air exchange rate to weaken the vertical temperature stratification, can keep the lock-up layer of the airborne aerosols away from human respiratory heights.

5. Conclusions

In this work, the impact of indoor thermal stratification on the dynamics of exhaled droplets while speaking is explored by theoretical analyses. It is confirmed that small droplets of <80μm evaporate and large droplets of >180μm fall to the ground rapidly within a close distance of 1.5 m, and are less affected by thermal stratification. However, the residues of small droplets remain airborne and can be carried over a long distance by the exhaled airflow when people are speaking, much more than 2m. In the calculations, the thermal stratification shows a significant impact on two aspects of the transmission of infectious diseases. In a thermally-stratified indoor environment, the droplet nuclei can be trapped at a certain height and penetrate over long horizontal distances. The lock-up height of the droplet nuclei is jointly determined by the temperature gradient and the droplet initial size in a power law. A large temperature gradient can make the droplet nuclei with a large size become locked at a low height close to people's breathing zone, so increasing the exposure risk to droplet nuclei over a long distance. But at the same time, a large temperature gradient can postpone the evaporation and accelerate the deposition of medium droplets, as a result, more droplets will deposit to the ground, decreasing the exposure to large droplets in close proximity to the source.

For medium droplets of 80-180μm, a high RH works equivalently to a large temperature gradient. Both the factors can reduce the number of droplets that would be inhaled by a person within a distance of 1.5m from the source. However, the dispersion of small droplets and droplet nuclei shows no dependence on RH, different from the behaviors with thermal stratification. The long-range dispersion and lock-up phenomena of the droplet nuclei should receive more attention in the control of airborne transmission when thermal stratification exists indoors. These findings are expected to be useful for developing engineering methods to control

infectious disease transmission via large droplets or airborne routes.

6. Limitations

There are some limitations to the current study. The exhalation flow is simplified to be steady in calculations; however, a realistic exhalation activity, such as coughing, is transient and generally characterized as a starting jet and an interrupted jet[13]. The shape of the mouth is treated as circular, without considering the impact of cavity shapes. These may produce slightly modified results, which need to be explored with further detailed studies in the future. In addition, respiratory droplets originating from the respiratory tract have different components such as virus and bacteria, which are neglected in the present models but can be expected to affect the evaporation process of droplets.

Finally, the present work is only focused on the dispersion of exhaled droplets and droplet nuclei; however, the transmission risk of respiratory diseases is also determined by many biological factors, such as viral kinetics (viral load and survival characteristics) in droplets, aerosol deposition efficiency in respiratory systems and the viral dose-response effect. Both the physical and biological factors should be considered when assessing disease transmission probability in any following work.

Acknowledgements

This work was supported by the National Natural Science Foundation of China (No. 51778128) and the Scientific Research Foundation of the Graduate School of Southeast University (No. YBJJ1806). The first author (F. Liu) would like to thank the financial support of the China Scholarship Council (CSC) for the academic visit at the University of Reading, where the

research was conducted.

Author Contributions

H. Qian, Z. Luo, X. Zheng contributed to the study design, hypothesis formulation, and coordination. F. Liu contributed to modelling and numerical simulation. F. Liu, H. Qian, Z. Luo contributed to the analyses. F. Liu wrote the first draft of the paper. All other authors contributed to the revisions.

Conflict of Interest Statement

The authors declare that no conflicts of interest exist.

All of the authors approved the submitted version and have agreed to be personally accountable for their own contributions.

References

1 Rota PA, Oberste MS, Monroe SS, *et al*. Characterization of a novel coronavirus associated with severe acute respiratory syndrome. *Science.* 2003;300 (5624):1394-1399.

2 Wolfe ND, Dunavan CP, Diamond J. Origins of major human infectious diseases. *Nature.* 2007;447:279-283.

3 Memish ZA, Cotten M, Meyer B, *et al*. Human infection with MERS coronavirus after exposure to infected camels, Saudi Arabia, 2013. *Emerg Infect Dis.* 2014;20(6):1012-1015.

4 Wu F, Zhao S, Yu B, *et al*. A new coronavirus associated with human respiratory disease in China. *Nature.* 2020;579:265-269.

5 Zhou P, Yang X, Wang X, *et al*. A pneumonia outbreak associated with a new coronavirus

of probable bat origin. *Nature.* 2020;579:270-273.

6 Lindsley WG, Reynolds JS, Szalajda JV, *et al*. A cough aerosol simulator for the study of disease transmission by human cough-generated aerosols. *Aerosol Sci Tech.* 2013;47(8):937-944.

7 Bourouiba L, Dehandschoewercker E, Bush JWM. Violent expiratory events: On coughing and sneezing. *J Fluid Mech.* 2014;745:537-563.

8 Duguid JP. The size and the duration of air-carriage of expiratory droplets and droplet-nuclei. *J Hyg.* 1946;44:471-479.

9 Hu Z, Song C, Xu C, *et al*. Clinical characteristics of 24 asymptomatic infections with COVID-19 screened among close contacts in Nanjing, China. *Sci China Life Sci.* 2020;63:1-6.

10 Rothe C, Schunk M, Sothmann P, *et al*. Transmission of 2019-nCoV infection from anasymptomatic contact in Germany. *New Engl J Med.* 2020;382(10):970-971.

11 Li R, Pei S, Chen B, *et al*. Substantial undocumented infection facilitates the rapid dissemination of novel coronavirus (SARS-CoV-2). *Science.* 2020;368(6490):489-493

12 Liu L, Li Y, Nielsen PV, *et al*. Short-range airborne transmission of expiratory droplets between two people. *Indoor Air.* 2016;27(2):452-462.

13 Wei J, Li Y. Enhanced spread of expiratory droplets by turbulence in a cough jet. *Build Environ.* 2015;93:86-96.

14 Xie X, Li Y, Chwang ATY, *et al*. How far droplets can move in indoor environments-revisiting the Wells evaporation-falling curve. *Indoor Air.* 2007;17(3):211-225.

15 Redrow J, Mao S, Celik I, *et al*. Modeling the evaporation and dispersion of airborne sputum droplets expelled from a human cough. *Build Environ.* 2011;46:2042-2051.

16 Brohus H, Nielsen PV. Personal exposure in displacement ventilated rooms. *Indoor Air*. 1996;6:157-167.

17 Bjørn E, Nielsen PV. Dispersal of exhaled air and personal exposure in displacement ventilated rooms. *Indoor Air*. 2002;12(3):147-164.

18 Qian H, Li Y, Nielsen PV, *et al*. Dispersion of exhalation pollutants in a two-bed hospital ward with a downward ventilation system. *Build Environ.* 2008;43:344-354.

19 Nielsen P, Olmedo I, Adana MR, *et al*. Airborne cross-infection risk between two people standing in surroundings with a vertical temperature gradient. *HVAC & R Res*. 2012;18(4):552-561.

20 Wei J, Li Y. Human cough as a two-stage jet and its role in particle transport. *PLoS One*. 2017;12(1):e0169235.

21 Liu F, Qian H, Luo Z, *et al*. A laboratory study of the expiratory airflow and particle dispersion in the stratified indoor environment. *Build Environ.* 2020;180:106988,

22 Qian H, Li Y, Nielsen PV, *et al*. Spatial distribution of infection risk of SARS transmission in a hospital ward. *Build Environ.* 2009;44:1651-1658.

23 Gupta JK, Lin CH, Chen Q. Characterizing exhaled airflow from breathing and talking. *Indoor Air*. 2010;20:31-39.

24 Ji Y, Qian H, Ye J, *et al*. The impact of ambient humidity on the evaporation and dispersion of exhaled breathing droplets: A numerical investigation. *J Aerosol Sci.* 2018;115:164-172.

25 Gao NP, Niu JL, Morawska L. Distribution of respiratory droplets in enclosed environment under different air distribution methods. *Build Simul.* 2008;1:326-335.

26 Li X, Niu J, Gao N. Spatial distribution of human respiratory droplet residuals and exposure

risk for the co-occupant under different ventilation methods. *HVAC&R Res.* 2011;17:432-445.

27 Qian H, Li Y, Nielsen PV, *et al*. Dispersion of exhaled droplet nuclei in a two-bed hospital ward with three different ventilation systems. *Indoor Air.* 2006;16:111-128.

28 Gao NP, Niu JL. CFD study of the thermal environment around a human body: A review. *Indoor Built Environ.* 2005;14(1):5-16.

29 Murakami S. Analysis and design of micro-climate around the human body with respiration by CFD. *Indoor Air.* 2010;14(S7):144-156.

30 Liu F, Zhang C, Qian H, *et al*. Direct or indirect exposure of exhaled contaminants in stratified environments using an integral model of an expiratory jet. *Indoor Air.* 2019;29(4):591-603.

31 Gilani S, Montazeri H, Blocken B. CFD simulation of stratified indoor environment in displacement ventilation: Validation and sensitivity analysis. *Build Environ.* 2016;95:299-313.

32 Gil-Lopez T, Galvez-Huerta MA, O'Donohoe PG, *et al*. Analysis of the influence of the return position in the vertical temperature gradient in displacement ventilation systems for large halls. *Energy Build.* 2017;140:371-379.

33 Kong Q, Yu B. Numerical study on temperature stratification in a room with under floor air distribution system. *Energy Build.* 2008;40:495-502.

34 Wang X, Huang C, Cao W, *et al*. Experimental study on indoor thermal stratification in large space by under floor air distribution system (UFAD) in summer. *Engineering.* 2011;3:384-388.

35 Menchaca-Brandan MA. Study of airflow and thermal stratification in naturally ventilated rooms (Ph.D. Thesis). Massachusetts Institute of Technology. 2012.

36 Dominguez-Espinosa FA, Glicksman LR. Determining thermal stratification in rooms with high supply momentum. *Build Environ.* 2017;112:99-114.

37 Gao N, He Q, Niu J. Numerical study of the lock-up phenomenon of human exhaled droplets under a displacement ventilated room. *Build Simul.* 2012;5:51-60.

38 Zhou Q, Qian H, Ren H, *et al*. The lock-up phenomenon of exhaled flow in a stable thermally-stratified indoor environment. *Build Environ.* 2017;116:246-256.

39 Mangili A, Gendreau MA. Transmission of infectious diseases during commercial air travel. *Lancet*. 2005;365:989-996.

40 Xiao S, Li Y, Sung M, *et al*. A study of the probable transmission routes of MERS-CoV during the first hospital outbreak in the Republic of Korea. *Indoor Air*. 2018;28(1):51-63.

41 Wells WF. On air-borne infection. Study II. Droplets and droplet nuclei. *Am J Hyg.* 1934;20:611-618.

42 Liu L, Wei J, Li Y, *et al*. Evaporation and dispersion of respiratory droplets from coughing. *Indoor Air.* 2017;27(1):179-190.

43 Chen W, Zhang N, Wei J, *et al*. Short-range airborne route dominates exposure of respiratory infection during close contact. *Build Environ.* 2020;176:106859.

44 Sami S, Carmody T, Rouse H. Jet diffusion in the region of flow establishment. *J Fluid Mech.* 1967;23:231-252.

45 Fan LN. Turbulent buoyant jets into stratified or flowing ambient fluids. *Report KH-R-15*. California Inst. of Technology, Pasadena, California, USA. 1967. 196p.

46 Chu PCK. Mixing of Turbulent Advected Line Puffs. Ph.D. Thesis. University of HongKong. 1996.

47 Jirka GH. Model for turbulent buoyant jets in unbounded stratified flows. Part I: Single Round Jet. *Environ Fluid Mech.* 2004;4:1-56.

48 Xiang HW. The new simple extended corresponding-states principle: Vapor pressure and second virial coefficient. *Chem Eng Sci.* 2002;57(8):1439-1449.

49 Chao CYH, Wan MP, Morawska L, *et al*. Characterization of expiration air jets and droplet size distributions immediately at the mouth opening. *J Aerosol Sci.* 2009;40(2):122-133.

50 Popov TA , Dunev S, Kralimarkova TZ, *et al*. Evaluation of a simple, potentially individual device for exhaled breath temperature measurement. *Resp Med.* 2007;101(10):2044-2050.

51 Smolík J, Džumbová L, Schwarz J, *et al*. Evaporation of ventilated water droplet: connection between heat and mass transfer. *J Aerosol Sci.* 2001;32(6):739-748.

52 Wang B, Zhang A, Sun JL, *et al*. Study of SARS transmission via liquid droplets in air. *J Biomech Eng.* 2005; 127: 32-38.

53 Gupta JK, Lin CH, Chen Q. Flow dynamics and characterization of a cough. *Indoor Air*. 2009;19:517-525.

54 BBC. Coronavirus: Could social distancing of less than two metres work? https://www.bbc.co.uk/news/science-environment-52522460 Accessed June 19, 2020.

55 Qian M, Jiang J. COVID-19 and social distancing. *Z Gesundh Wiss.* 2020;1-3.

56 Scottish Government. Coronavirus (COVID-19): guidance 2020. https://hpspubsrepo.blob.core.windows.net/hps-website/nss/2973/documents/1_covid-19-guidance-for-non-healthcare-settings.pdf Accessed June 19, 2020.

57 Hinds WC. Aerosol technology: properties, behavior, and measurement of airborne particles. John Wiley & Sons, New York; 1999. 233-245p.

58 Carvalho TC, Peters JI, Williams III RO. Influence of particle size on regional lung deposition-what evidence is there? *Int J Pharm.* 2011;406(1-2):1-10.